

ON THE RATIONAL DESIGN OF COMPRESSIBLE FLOW EJECTORS

P. J. Ortwerth

Chemical Laser Branch, Air Force Weapons Laboratory
Kirtland Air Force Base, New Mexico

SUMMARY

A fluid mechanics review of modern ejectors has identified the following parameters that must be considered when designing ejectors for a chemical laser pressure recovery system. The first parameter is called the secondary flow admittance, or inversely the flow impedance, defined as the ratio of secondary mass flow and secondary total pressure. The laser diffuser critical pressure recovery defines the ejector input impedance. Internally the ejector suction characteristics define an ejector impedance. The first design condition to be met is the secondary flow impedance matching condition. The second important characteristic is the secondary flow Mach number. The secondary flow Mach number is found to have an important influence on ejector performance for low mass ratio and should be optimized for the design operating point. The last critical parameter is the ejector throat area. The ejector area insures that impedance is matched correctly and the desired performance obtained. The throat area depends very strongly on the distortion produced by the dynamics of the mixing layer of primary and secondary flow. If the application permits, multiple driver nozzles can be used to minimize distortion which results in the maximum performance of the pressure recovery system.

1. INTRODUCTION

In the application of CW chemical lasers to military systems the ejector plays a critical role. The optimization of the ejector is important in reducing the weight and volume of the system. The ejector is normally the largest component of the laser device and consumes several times as much propellant as the laser cavity. An integrated laser diffuser ejector schematic is shown in figure 1 for comparing size and defining components. Research in ejector fluid mechanics has been largely experimental and a large body of relevant data is now available (refs. 1-4). These data must be exploited fully in order to reduce the time and expense of building future large systems. It is the purpose of this paper to explain the characteristics of the ejector from an elementary fluid mechanics approach. A modern ejector is defined as one in which the secondary Mach number is chosen to optimize performance, as opposed to previous designs where it is assumed that $M_s = 0.2$. It is desirable to avoid relying on purely empirical correlation of the data since such attempts have been known to fail in the past when scales and the primary and secondary flow properties have varied significantly.

II. REVIEW OF SELECTED EJECTOR PROPERTIES

As a prelude to developing the method and theory of ejector design we shall review selected ejector experimental data which are important for understanding the fluid mechanics of good ejectors.

Existence of a Critical Point

The data in figure 2 shows how the inlet pressure in the ejector varies with the back pressure. Two regions exist: the supercritical region at low back pressure in which the inlet pressure is constant independent of back pressure, and the subcritical region in which back pressure determines inlet pressure. The point separating these two regions is called the critical point. While chemical laser diffuser ejectors systems have operated in the subcritical ejector range, it is undesirable for the impedance to depend on back pressure. Highest efficiency of the diffuser ejector system is obtained when the diffuser and ejector operate at their respective critical points. For assured safe operation it is desirable to design both the diffuser and ejector at slightly supercritical conditions. A good design methodology must be able to predict the critical point for all operating conditions of the laser.

Supercritical Pressure Distribution

Let us examine the effect of back pressure on the axial pressure distribution in the ejector. The data in figure 3 shows a constant pressure distribution independent of back pressure in the mixing section. Downstream after the throat station, the pressure distribution is determined by back pressure in exactly the same way as back pressure affects supersonic diffusers. The critical point is reached when the shock structure has moved to the throat of the ejector. It is exactly these features which make the determination of the critical point a priori possible by applying standard flow conservation analysis.

Throat Flow Distortion and Mixing

The one-dimensional analysis of ejectors requires the flow be completely mixed at the throat. However, pitot-pressure profiles in the throat of an ejector are very distorted as shown in figure 4. Clearly, a longer mixing section would be required to completely mix the flow. A longer mixing section is definitely not desired, however, since that would only add to the weight and volume of the ejector. In fact the profiles in figure 4 correspond to the operating conditions of figure 3 in which critical operation was achieved at satisfactory performance level for many applications. A very important feature of these profiles is that the mixing zone has reached the wall as evidenced by the positive slope of the pitot profiles from the wall. This feature is important to achieve critical operation since the low momentum secondary flow cannot undergo compression unless shear forces are present to balance

the pressure gradient. Ideal calculations discussed later show the completely mixed flow would occupy an area 73% as large as the real area and performance would be 30% higher. We conclude that distortion is responsible for a significant correction to real ejector throat area requirements and, therefore, performance.

Existence of Ejector Flow Impedance and Impedance Matching with Diffusers

While most ejector characteristics are best presented in nondimensional coordinates the existence of flow impedance is readily recognized in dimensional coordinates. The data (ref. 2) for secondary flow rate versus secondary pressure commonly called the suction characteristics clearly show that for a wide range of conditions the secondary mass flow is dependent on secondary total pressure only (fig. 5). In fig. 5, the significant primary mass flow and nozzle diameter variations shown in the legend do not affect the linear relationship of secondary mass flow with secondary total pressure. The common practice of normalizing this curve by primary mass flow and pressure is fictitious and misleading. We can then define an ejector admittance.

$$A = \frac{\dot{W}_s}{P_{0s}} \quad (1)$$

This relation states that the secondary volume flow rate is constant over all conditions tested. This amazing fact correlates with the only other fixed parameter in the tests which is the mixing length. The absolute entrainment rate is also only pressure dependent when the other shear layer conditions are fixed. Thus, based on the properties of entrainment, constant volume flow rate is to be expected and is observed. This feature is one of the chief virtues of an ejector that make it a true pumping system. For completeness, figure 6 is included for the accepted critical diffuser impedance characteristics as determined from experimental data.

Impedance Dependence on Mixing Length¹ (Minimum impedance and critical mixing length)

A very important phenomena is observed when the position of the primary driver nozzle is moved relative to the ejector throat inlet. As shown in figure 7 the secondary total pressure depends on the nozzle location under condition of fixed secondary flow rate. This means flow impedance will also depend on mixer geometry. There is a critical zone, between seven and eight nozzle diameters upstream of the throat, where impedance is a minimum. An explanation of this phenomena can be constructed based on the mixing dynamics of the primary and secondary flows. The reasoning is based on the observed pitot-pressure profile of figure 4 which was obtained when the nozzle was located in the critical mixing zone. As stated above, we identify the

¹The Impedance depends on mixer contraction cone angle (refs. 1, 3, and 4) but will not be discussed here.

critical zone with the condition that the shear layer has just entrained the last secondary flow streamline.

For shorter distances unmixed secondary flow must pass through the restrictive throat area requiring an increased secondary total pressure. While the longer mixing lengths, the potential core is mixed out and the shear layer greatly expands. The expanded mixing zone also has to be compressed to fit through the throat area.

The exit pressure maximizes at the same mixing length. One reason for this is that the drag of the mixing section is a minimum at this condition.

Critical Point Performance Dependent on Secondary Flow

The last feature we wish to review is the dependence of the ejector critical point performance secondary flow rate in figure 8. The data illustrates the fact that lowest exit pressure is achieved when the secondary flow is zero. Pressure increases monotonically with increasing secondary flow and is entirely consistent with a conservation analysis of the ejector performance.

This curve reveals design point operation requires less primary mass flow than start conditions. Recalling that secondary flow entrainment does not depend on primary pressure means that the ejector can be turned down as the laser starts without fear of unstarting the laser.

III. DESIGN METHOD

Several theoretical tools are necessary to cope with the variety of issues just discussed. Every design will start with a requirement to pump a secondary mass flow and total pressure delivered by the laser to the final exhaust pressure level. A wide variety of laser gas and primary gas properties are encountered.

The selection of a primary nozzle propellant will not be considered in this paper but clearly is important in a real application. Laser gas properties can also vary and, importantly, the gases may be cooled. The overall length may be a constraint and multiple ejectors side by side might be in order. All these issues and more do not directly relate to the fluid mechanics methodology. In the next section we will develop the tools for the following method:

1. A method to compute an optimized performance map in which secondary Mach number and performance are computed versus mass ratio.
2. A method to compute the flow distortion at each optimized condition. Performance is adjusted for the distortion losses and the design point is selected.

3. The throat area is determined for the design point to match diffuser impedance. Off design performance is then computed to match other facility or system requirements using a fixed geometry performance calculation.

Optimization of the Ideal Ejector Design

The question usually asked by the system designer is, "What is the lowest mass ratio needed to pump from diffuser exit pressure to ambient?" Theoretically it is simpler to ask the question, "what's the highest pressure ratio available for a given mass ratio?" We consider secondary flow rate, total pressure, and total temperature to be fixed initial conditions. We consider the primary flow rate, Mach number, total temperature to be fixed. The question is, "what control is available to optimize performance?" Before we answer this question we should review the factors affecting performance.

The ejector is a pump with two important processes, both of which are inherently lossy. The first is an entrainment by tangential shear stress at constant pressure and the second is a compression of the mixed gases. The compressor is a normal shock followed with subsonic diffuser.

What we seek is to minimize the total pressure losses in the mixing and compression processes. At high mass ratio mixing losses will be inherently small and the dominant losses will be normal shock losses, and the reverse is true at low mass ratios. We shall not consider subsonic diffuser losses in this optimization process for the following reasons.

First, the normal shock compression losses are dominant. Second, in practice, the subsonic diffuser is usually conical in shape and designed for the optimum angle of subsonic diffusers. The performance of the subsonic diffuser then depends on the inlet flow blockage only, according to Sovran and Klomp (ref. 5). For flow after a normal shock, we would expect blockage to be constant, independent of upstream conditions and thus the C_p of the diffuser will also be considered constant.

For simplicity then we shall optimize the ejector for maximum pressure after the normal shock. From this brief inspection of the problem it is clear only one input parameter left unspecified can affect the losses in any meaningful way and this is the secondary velocity or Mach number. First, the secondary flow velocity directly determines the mixing losses and the mixed gas Mach number and, thus, the normal shock losses. Secondly, the secondary static pressure is dependent on secondary Mach number which has a strong effect on throat area. We proceed as follows:

Let the normalized optimization parameter be

$$\theta = \frac{U_s}{U_p} \quad (2)$$

Then the mixed gas velocity will be

$$U_2 = U_p \left(\frac{\mu + \theta}{\mu + 1} \right) \quad (3)$$

where

$$\mu = \frac{\dot{W}_p}{\dot{W}_s} \quad (4)$$

is the ejector mass ratio. The mixed gas Mach number becomes

$$M_2^2 = \left(\frac{2}{\gamma - 1} \right) \left(\frac{U_2^2}{2H_2} \right) \left(1 - \frac{U_2^2}{2H_2} \right)^{-1} \quad (5)$$

The normal shock pressure ratio is thus dependent on the secondary static pressure and we write the function to be maximized in two parts:

$$\frac{P_3}{P_{os}} = \left(\frac{P_3}{P_2} \right)_{N.S.} \frac{P_2}{P_{os}} \quad (6)$$

where the normal shock pressure ratio

$$\left(\frac{P_3}{P_2} \right)_{N.S.} = \frac{2\gamma}{\gamma + 1} M_2^2 - \frac{\gamma - 1}{\gamma + 1} \quad (7)$$

and the secondary static pressure are dependent on θ .

$$\frac{P_2}{P_{os}} = \left(1 - \frac{U_s^2}{2H_s} \right)^{\gamma_s/\gamma_s-1} \quad (8)$$

Defining the following functions:

$$\theta_1 \equiv 1 + \frac{\theta}{\mu} \quad (9)$$

$$\theta_2 \equiv \theta_1^2 \quad (10)$$

and the following constants:

$$B \equiv \left(\frac{\mu}{1 + \mu} \right)^2 \frac{U_p^2}{2H_2} \quad (11)$$

$$A = \left(\frac{\gamma + 1}{\gamma - 1} \right)^2 B \quad (12)$$

$$\theta_m^2 = \frac{2H_s}{U_p^2} \quad (13)$$

we obtain

$$\frac{P_3}{P_{0s}} = - \left(\frac{\gamma - 1}{\gamma + 1} \right) \left(\frac{A\theta_2 - 1}{B\theta_2 - 1} \right) \left(1 - \frac{\theta^2}{\theta_m^2} \right)^{\gamma_s/\gamma_s-1} \quad (14)$$

To obtain the condition for the maximum performance we differentiate with respect to θ and set the derivative equal to zero.

$$\frac{d\left(\frac{P_3}{P_{0s}}\right)}{d\theta} = F(\theta) = \frac{\frac{2A}{\mu} \theta_1}{A\theta_2 - 1} - \frac{\frac{2B}{\mu} \theta_1}{B\theta_2 - 1} - \frac{\gamma_s - 1}{\gamma_s} \frac{2}{\theta} \quad (15)$$

This equation is solved numerically using a Newton-Raphson technique.

The variation of optimum secondary Mach number with mass ratio is shown in figure 9, from reference 6. At low mass ratio the secondary mass ratio increases to Mach 1 while at high mass ratio the results tend toward the classical rule of thumb secondary Mach number of 0.2. The importance of this parameter is shown in figure 10 also from reference 7, where a 50% increase in performance is obtained by doubling the secondary flow Mach number from the classical $M_s = 0.2$.

Calculation of the Admittance of the Ejector (Single Primary Nozzle)

In the previous discussion we found the best conditions for minimizing the ideal ejector losses. The ejector design will work only if the internal admittance of the ejector is matched to the requirements of the diffuser. The admittance is controlled by two factors the second throat area and the mixing section contraction and length. It is most important to be able to calculate the second throat area and we will proceed to formulate the solution to that problem. The mixer design requires the calculation of the absolute entrainment rate and is beyond the scope of the present paper.

The calculation of the area of the second throat for a single primary nozzle driver is based on the identification in the review section that admittance is optimized when the mixing zone just reaches the wall. In this case the flow consists of two regions: first, the potential core and, second, the shear layer. This condition is shown in figure 11. To calculate the area of the shear layer for the condition that all the secondary flow is entrained, we make the following simplifying assumptions for the profile, first that the turbulent Prandtl and Schmidt numbers are unity and second that the velocity profile can be approximated by a cosine law. We then proceed as follows:

Shear layer profiles are:

$$\text{Velocity} \quad \frac{U - U_s}{U_p - U_s} = \frac{1}{2} \left[1 + \cos\left(\frac{\pi Y}{h}\right) \right] \quad (16)$$

where

$$Y = (r - r_i) \quad (17)$$

and

$$h = (r_o - r_i) \quad (18)$$

Total enthalpy

$$\frac{H - H_s}{H_p - H_s} = \frac{U - U_s}{U_p - U_s} \quad (19)$$

Primary fluid mass fraction

$$Y_p = \frac{U - U_s}{U_p - U_s} \quad (20)$$

Secondary mass fraction

$$Y_s = 1 - Y_p \quad (21)$$

The conservation equations for the flows through the mixer are:

Continuity

$$\dot{W}_2 = 2\pi \int_0^{r_o} \rho u r dr - \dot{W}_p + \dot{W}_s \quad (22)$$

Thrust balance

$$F_2 = P_s \pi r_o^2 + 2\pi \int_0^{r_o} \rho u^2 r dr \quad (23)$$

and

$$F_2 = F_p + F_s - P_s (\pi r_s^2 - \pi r_o^2) \quad (24)$$

The static pressure P_s is computed from the admittance and optimum secondary Mach number. The stream thrust of the primary and secondary flows are computed from the one dimensional formula

$$F = PA(1 + \gamma M^2 \eta_F) \quad (25)$$

Energy balance

$$\dot{W}_2 H_2 = 2\pi \int_0^{r_o} \rho u H r dr \quad (26)$$

and

$$\dot{W}_2 H_2 = \dot{W}_p H_p + \dot{W}_s H_s \quad (27)$$

The energy equation is not needed for the solution since only two unknowns exist r_i and r_o . The energy equation is a useful check sum of the calculation.

Normalizing the equations facilitate solution letting

$$\tilde{r} = \frac{r}{r_p}, \quad \tilde{\rho} = \frac{\rho}{\rho_p}, \quad \tilde{U} = \frac{U}{U_p}, \quad \text{and} \quad \eta = \pi \frac{\tilde{Y}}{h} \quad (28)$$

We obtain a transformed continuity equation

$$\tilde{r}_1^2 + \frac{2\tilde{r}_1 \tilde{h}}{\pi} I_1 + \frac{2\tilde{h}^2}{\pi^2} I_2 = 1 + \frac{1}{\mu} \quad (29)$$

and transformed momentum equation

$$\tilde{r}_1^2 + \frac{2\tilde{r}_1 \tilde{h}}{\pi} I_3 + \frac{2\tilde{h}^2}{\pi^2} I_4 = 1 + \frac{\theta}{\mu} \quad (30)$$

where

$$I_1 = \int_0^\pi \tilde{\rho} \tilde{U} d\eta \quad (31)$$

$$I_2 = \int_0^\pi \tilde{\rho} \tilde{U} \eta d\eta \quad (32)$$

$$I_3 = \int_0^\pi \tilde{\rho} \tilde{U}^2 d\eta \quad (33)$$

$$I_4 = \int_0^\pi \tilde{\rho} \tilde{U}^2 \eta d\eta \quad (34)$$

The normalized continuity and thrust balance equation can be solved numerically by the Newton-Raphson method.

Fixed-Geometry Performance

We can calculate the ejector performance for any W_s by using the conservation equations since we know the ejector throat area and admittance.

Pressure after the shock is computed as follows. Through the shock duct the quantity

$$N \equiv \frac{\dot{W}_2}{F_2} \left(\frac{RT_t}{\gamma} \right)^{1/2} = \frac{M \left(1 + \frac{\gamma - 1}{2} M^2 \right)^{1/2}}{1 + \gamma M^2} \quad (35)$$

is conserved. We can solve this equation explicitly for Mach number after shock

$$M_3 = \left(\frac{K - \sqrt{K - 2N^2}}{1 - \gamma K} \right)^{1/2} \quad (36)$$

where

$$K = 1 - 2\gamma N^2 \quad (37)$$

we find pressure after shock from the formula

$$P_3 = \frac{F_2/A_2}{1 + \gamma M_3^2} \quad (38)$$

This somewhat tedious method of computation does not require matched primary nozzle exit pressure and secondary static pressure. It also correctly accounts for the larger area due to distortion. Thus, this analysis is aptly suited for fixed geometry off design calculations.

We can compute ejector-off design performance since the admittance allows us to calculate P_{os} for any W_s and all other parameters are known including θ which is also constant.

The Critical Mass Ratio

The condition $r_i = 0$ represents the last condition for which the ejector falls in the high performance classification. Throat distortion rapidly increases at lower mass ratios and the required throat area also increases rapidly. The condition is

$$\mu_{\min} = \left(1 - \theta \frac{I_2}{I_4} \right) \left(\frac{I_2}{I_4} - 1 \right)^{-1} \quad (39)$$

Comparison of Theoretical and Experimental Ejector Results

Design point characteristics of the single-driven nozzle tested at UTRC by Zumpano (ref. 1) are shown in table 1.

Overall agreement between the theoretical and experimental ejector designs is very good. Particularly important is the power of using the distorted profile for determining the actual ejector throat area. This throat area is critical to insuring the admittance is determined correctly and we can compute the off-design performance. The entire operating range of the ejector is shown in figure 12 and compared with the fixed-geometry calculation using constant admittance. Also shown is the ideal performance computed for the one-dimensional throat area. This performance deficit between the ideal performance and the real performance dramatically illustrates the improvement available by eliminating the flow distortion.

While it is probably obvious that these results are not universal, note that for every different choice of initial conditions the ejector design and performance will be different.

Summary of Single-Nozzle Designs

Before considering ejectors with multiple-drive nozzles let us summarize what we can do up to this point.

1. Calculate the second throat area for any design point that matches the secondary flow admittance with ejector admittance.
2. Find the ejector with the minimum mass ratio for the design pressure ratio.
3. Since area and admittance are known we can compute off-design performance down to the critical mass ratio.

Multiple-Injector Nozzles

We shall now discuss a heuristic method for determining the number of primary nozzles necessary to reduce the distortion of the flow. Reducing the distortion means we can invoke the condition,

$$A_t = A_{ideal} \quad (\text{at the design point}) \quad (40)$$

First let us reexamine the two profiles with minimum distortion. In the ideal case of uniform profiles no distortion exists. In the second case, distortion is minimized when the mixing zone just reaches the wall, as in figure 13(a).

A feature of note is the existence core with very high mass flux. This feature is crucial in minimizing the overall distortion.

Now let us consider the following series of overlapping mixing zones² obtained by using multiple nozzles. As the geometry of the mixing zones show,

²This particular example is for Air-Air mixing at a mass ratio of 3.6.

the first case tested in which the mixing zones do not destroy the core flow is the case for five nozzles (fig. 13(e)). Based on the geometry of mixing zone overlap in figure 13 we have a criteria:

"The minimum number of primary nozzles required to achieve ideal area ratio is that number for which the mixing zones of adjacent nozzles just osculate the potential core."

That this criteria is borne out in practice is demonstrated by the data of figure 14 in which ejector performance is compared for 1, 4, and 7 nozzles. The performance of the single nozzle and the four nozzle drivers is practically the same while a significant increase in performance is observed for the 7-nozzle driver. A similar improvement was noted for the 5-nozzle driver over the single-nozzle driver of reference 1.

Nonconstant Admittance of Multiple-Driver Nozzles

Multiple-driver nozzles now enjoy the condition

$$A_{\text{real}} = A_{\text{ideal}} \quad (\text{design point}) \quad (41)$$

whereas single-driver nozzles are required to operate with

$$A_{\text{real}} > A_{\text{ideal}} \quad (42)$$

Unfortunately the condition of constant admittance cannot be fulfilled at all off-design conditions since the condition

$$A_{\text{real}} < A_{\text{ideal}} \quad (\text{off design}) \quad (43)$$

occurs in theory but in practice area is fixed in steel. Because of this, another adjustment in operation is observed. This effect is shown in figures 15 and 16 for the five nozzle primary driver steam ejector system of reference 4.

In figures 15 and 16 the curves labeled 1 show the behavior of the mass flow and area for the constant admittance condition. We can see the ideal area required increases as the ejector operates off the design secondary mass flow point. By applying the condition that

$$\frac{(\text{Pos})_r A_{\text{real}}}{(\text{Pos})_i A_{\text{ideal}}} = 1 \quad (44)$$

the curves labeled 2 can be constructed giving a variable admittance which does in fact reproduce the data point at $W_s = 0.1 \text{ lbm}$. The way in which this behavior influences the performance data is shown in figure 17.

CONCLUSIONS

An elementary fluid mechanics analysis of chemical laser ejectors has been accomplished. This analysis has been successful in explaining the characteristics of ejectors with single- and multiple-driver nozzles. As a result a rational methodology has been developed which can be applied to design the optimum ejector for specific application requirements without recourse to unreliable empirical formulas.

REFERENCES

1. Kepler, C. E.; Zumpano, F. R.; Landerman, A. A.; Biancardi, F. R.; Brooks, C. S.; and Russell, S: Pressure Recovery/Scrubber Systems for Chemical Lasers. Naval Surface Weapons Center, White Oak, Silver Spring, MD, Technical Report R75-911976-82, March 1975.
2. Teper, R.: Chemical Laser Ejector Demonstration. Air Force Weapons Laboratory, Technical Report AFWL-TR-76-92, Dec. 1976.
3. Teper, R. I.; and Arbit, H. A., Chemical Laser Advanced Diffuser/Ejector. Final Report, US Army Missile R&D Command Redstone Arsenal, Alabama, Report No. RI/RD 78-102, Jan. 1978.
4. Biancardi, F. R.; Landerman, A. M.; Melikian, G.; Schulman, E. R.; and Zumpano, F. R.: Design and Development of a Compact Pressure Recovery/Scrubber System for Chemical Lasers. Naval Sea Systems Command, PMS 405, Arlington, VA, Technical Report R76-952406, Nov. 1976.
5. Sovran, G.; and Klomp, E. D.: Experimentally Determined Optimum Geometries for Rectangular Diffusers with Rectangular, Conical or Annular Cross Section, Fluid Mechanics of Internal Flow, ed. Sovran, G., Elsevier Publishing Company, Amsterdam, 1967.
6. Ortwerth, P. J.: On Ejector Optimization. Laser Digest-Spring 1976, Air Force Weapons Laboratory Technical Report AFWL TR 76-131, 1976.

TABLE 1.- COMPARISON OF DESIGN POINTS FOR SINGLE-DRIVER NOZZLE (AIR/AIR)

	Mp	$\alpha^{1/2}$	μ	θ	Ms	A_t/A_n	A^a	$(P_e/P_{0s})_{crit}$	μ_{crit}^b
Experiment	4.46	15°	3.6	---	---	4.59	66.7	5.2 ^d	1.5 ^b
Theory	4.3 ^c	0	3.6	0.21	0.42	4.60	67.7	5.2 ^d	1.4
Theory	4.46	0	3.6	.21	.42	4.78	67.7	5.3 ^d	1.4

^aNormalized admittance (see fig. 8).

^bLast experimental data point given and presumed to be near breakdown.

^cNozzle Mach number with same thrust as M = 4.6 nozzle with 15° divergence losses.

^dPerformance computed assumes subsonic diffuser $C_p = 0.7$.

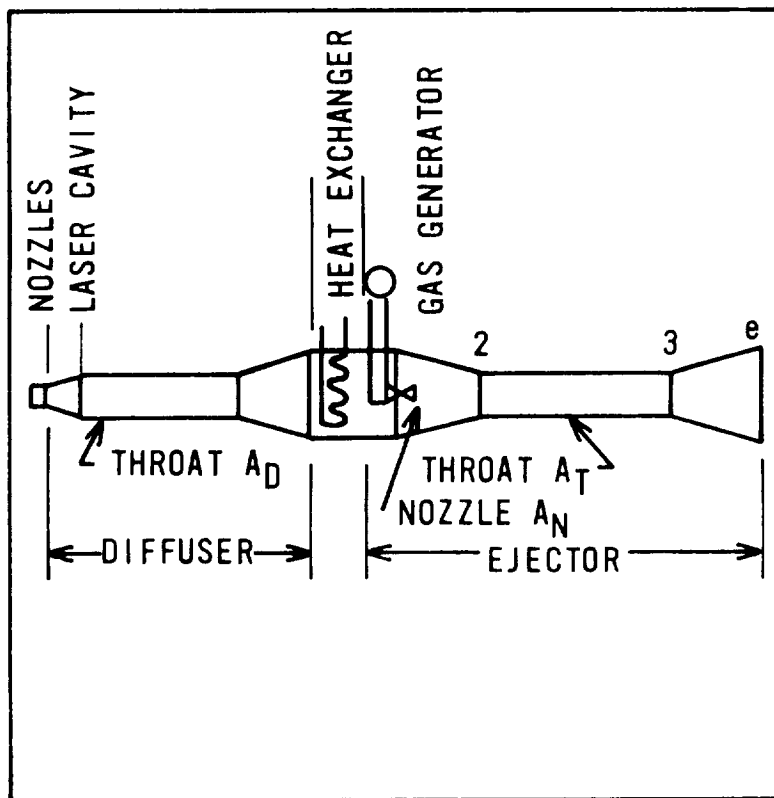


Figure 1.- Chemical laser pressure recovery system.

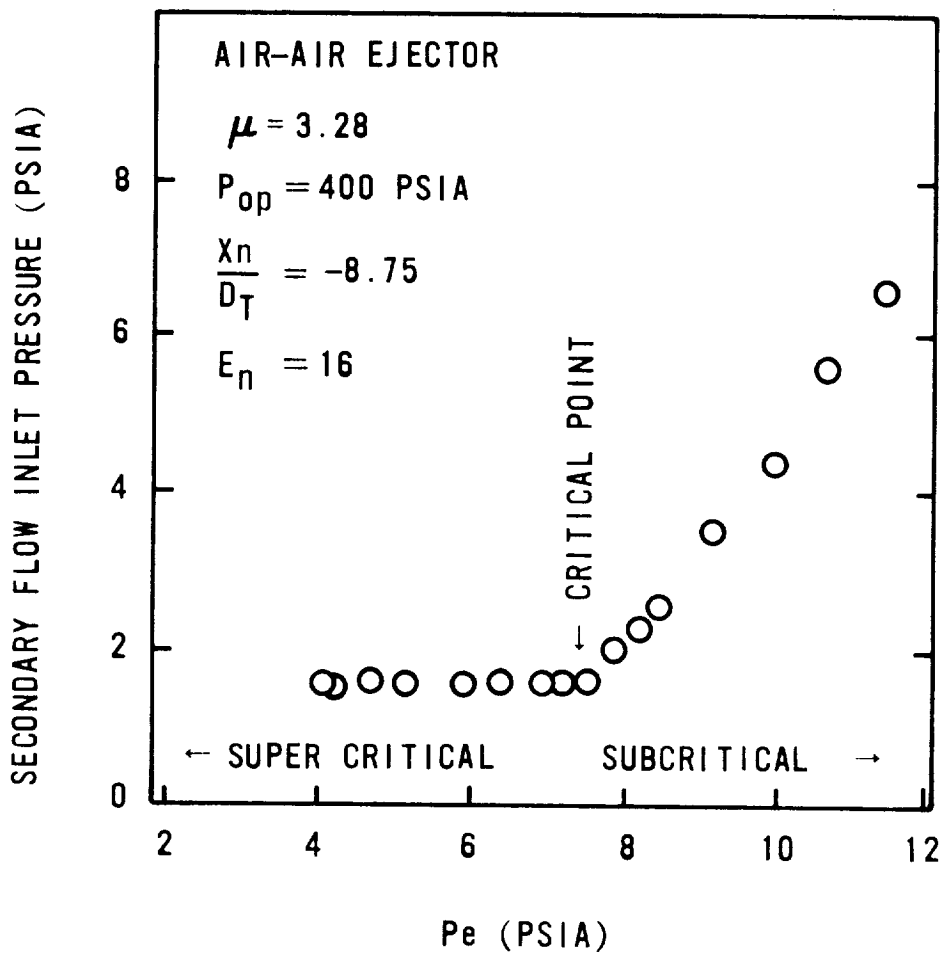


Figure 2.- Ejector operating conditions.

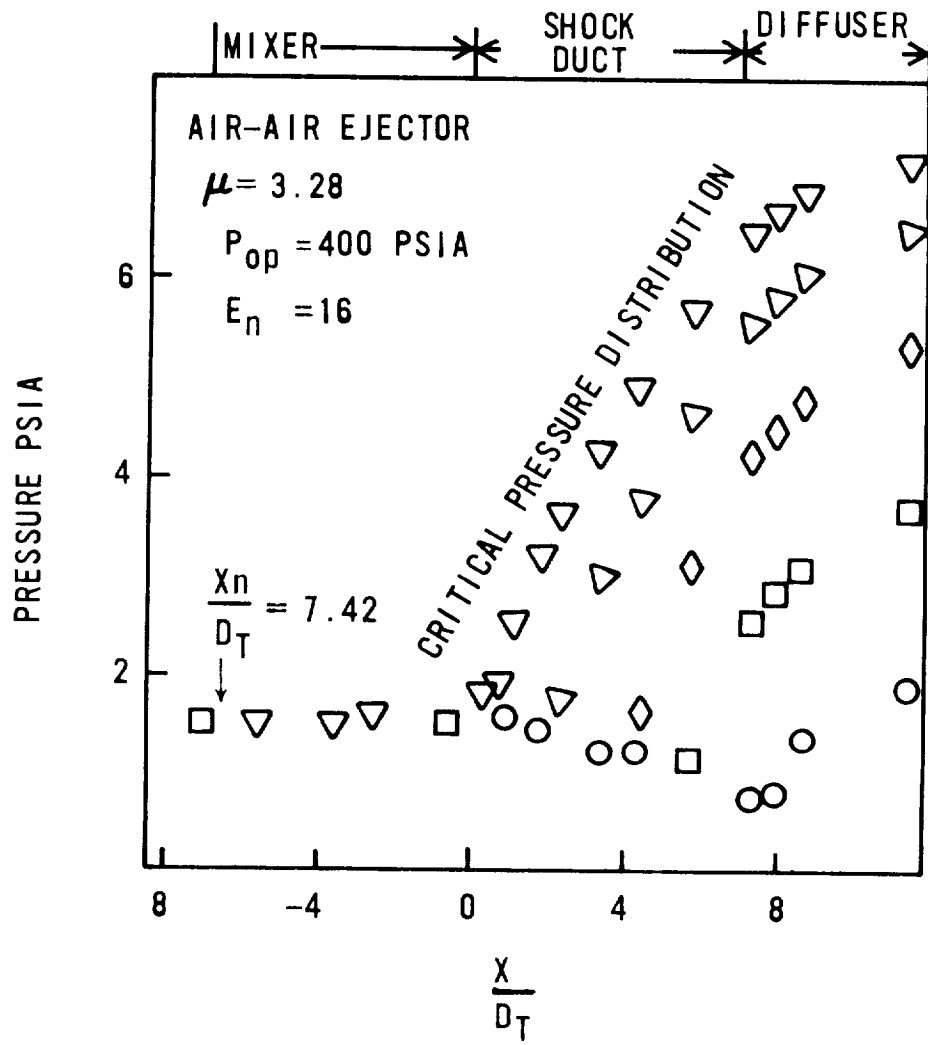


Figure 3.- Ejector axial pressure distributions.

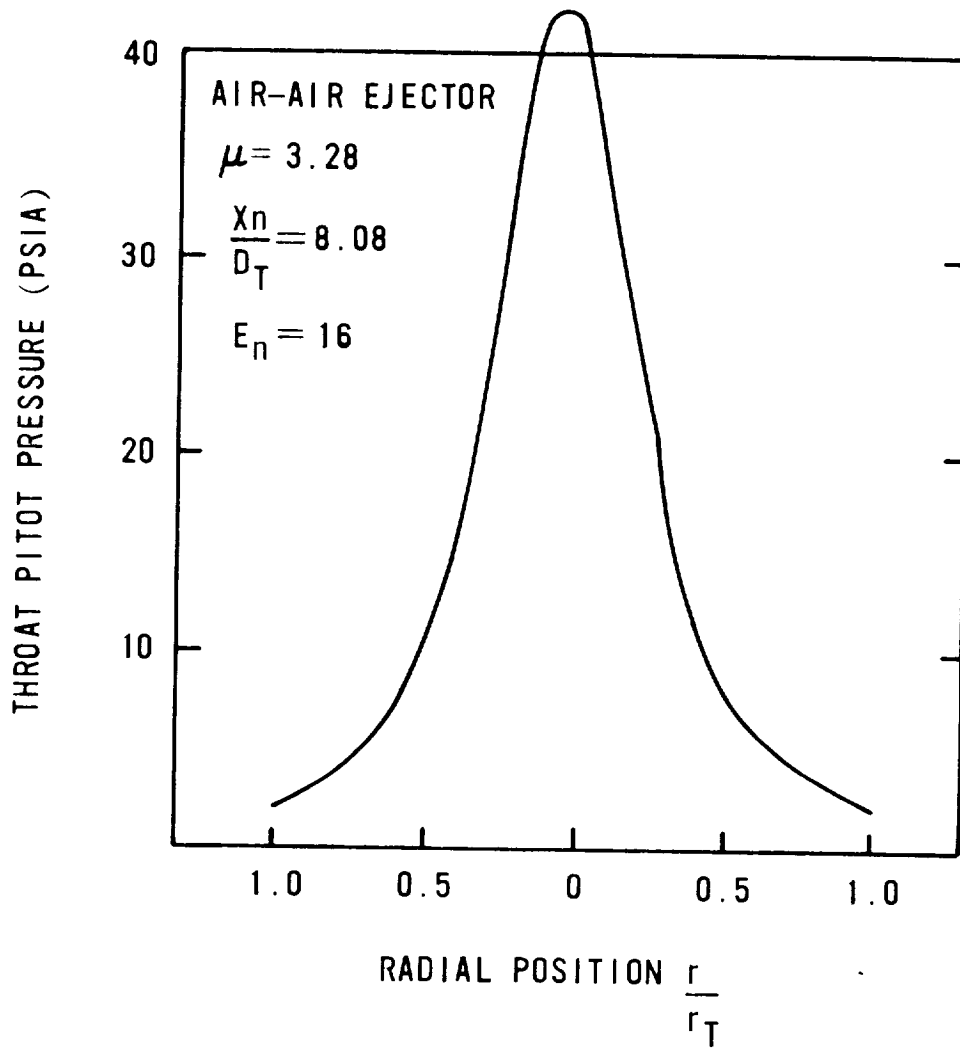


Figure 4.- Ejector throat pitot profile.

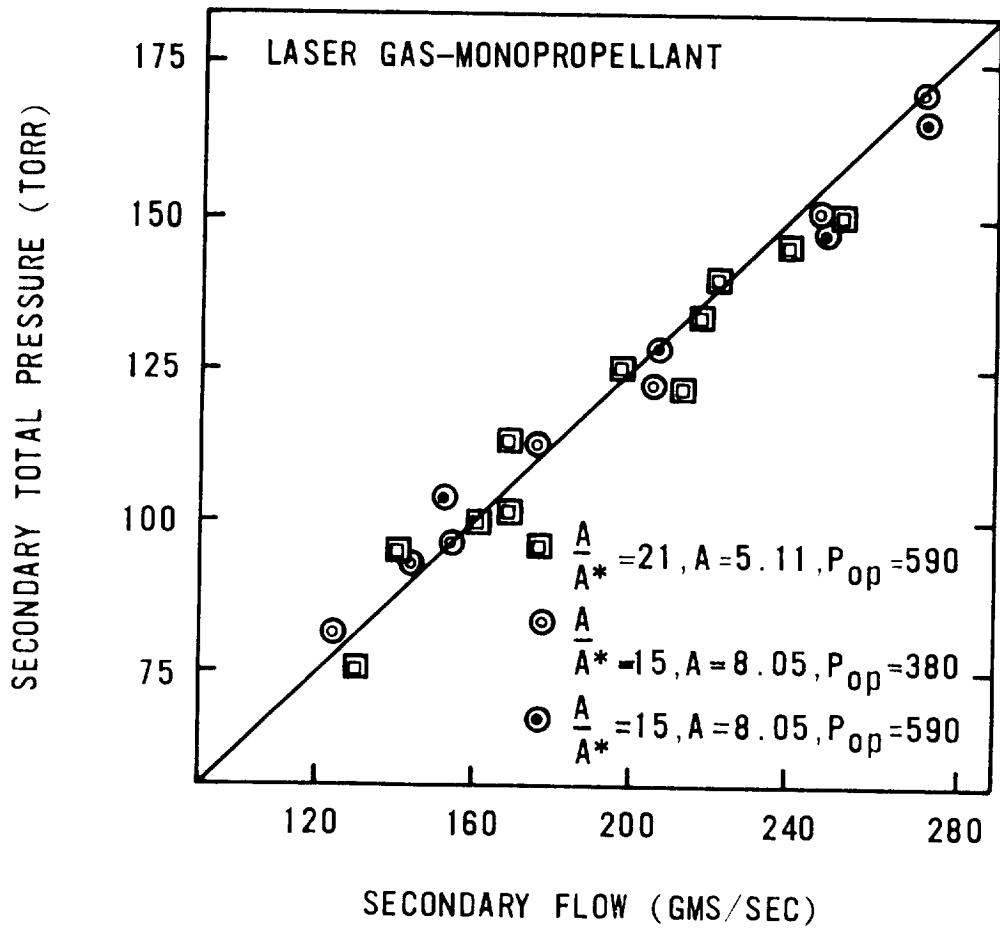


Figure 5.- Ejector suction characteristics.

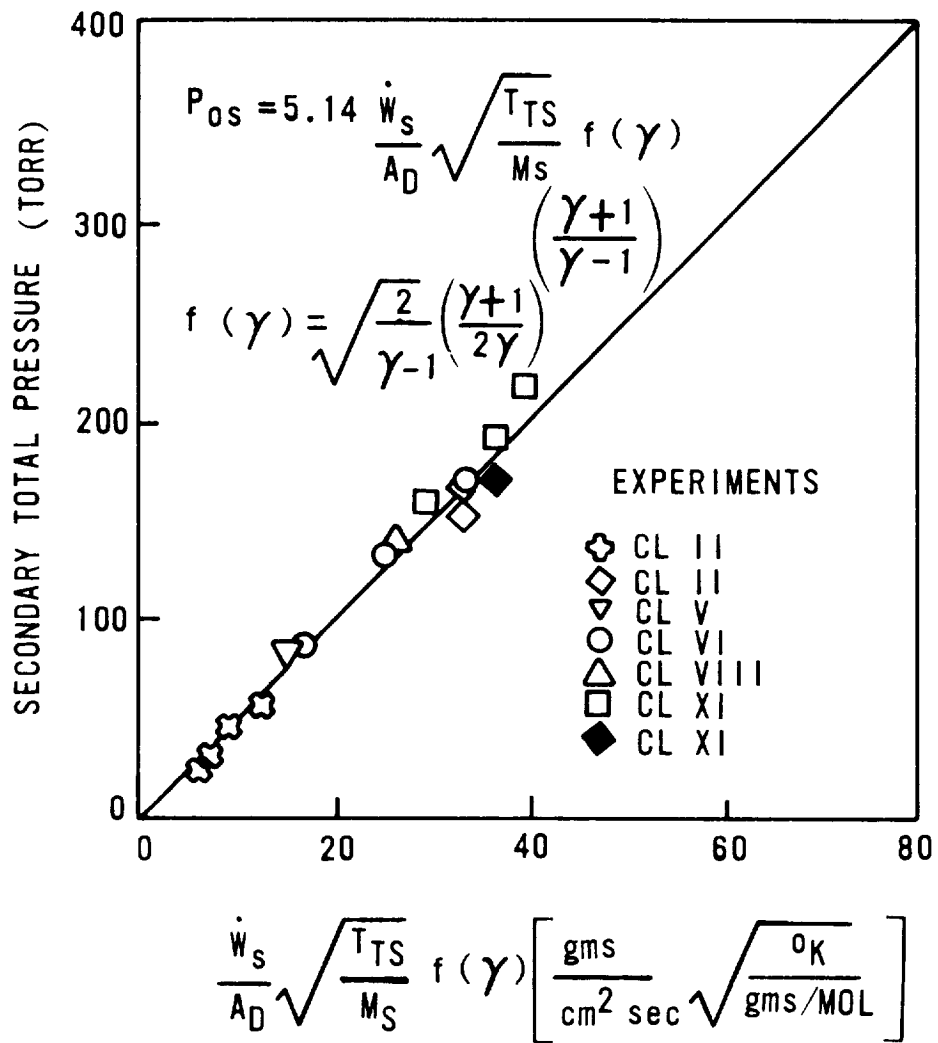


Figure 6.- Diffuser critical pressure recovery.

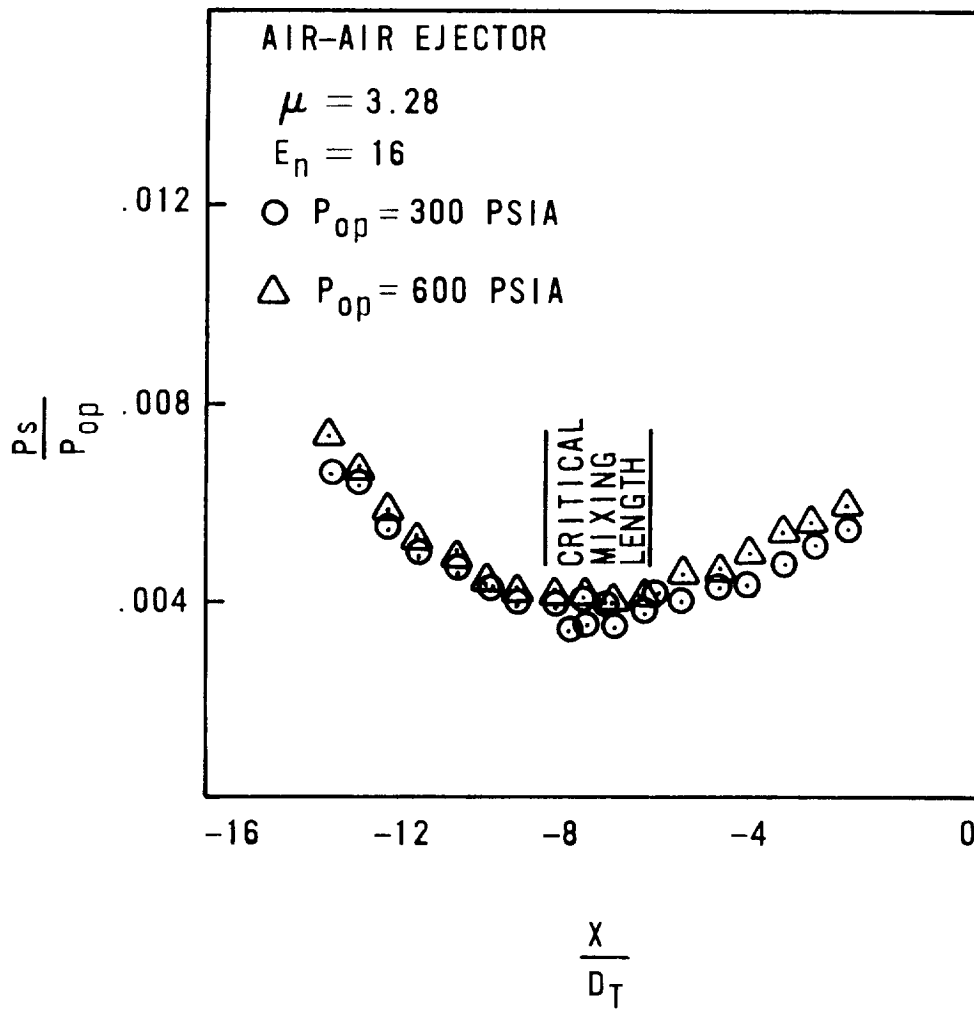


Figure 7.- Effect of mixing length on ejector suction characteristics.

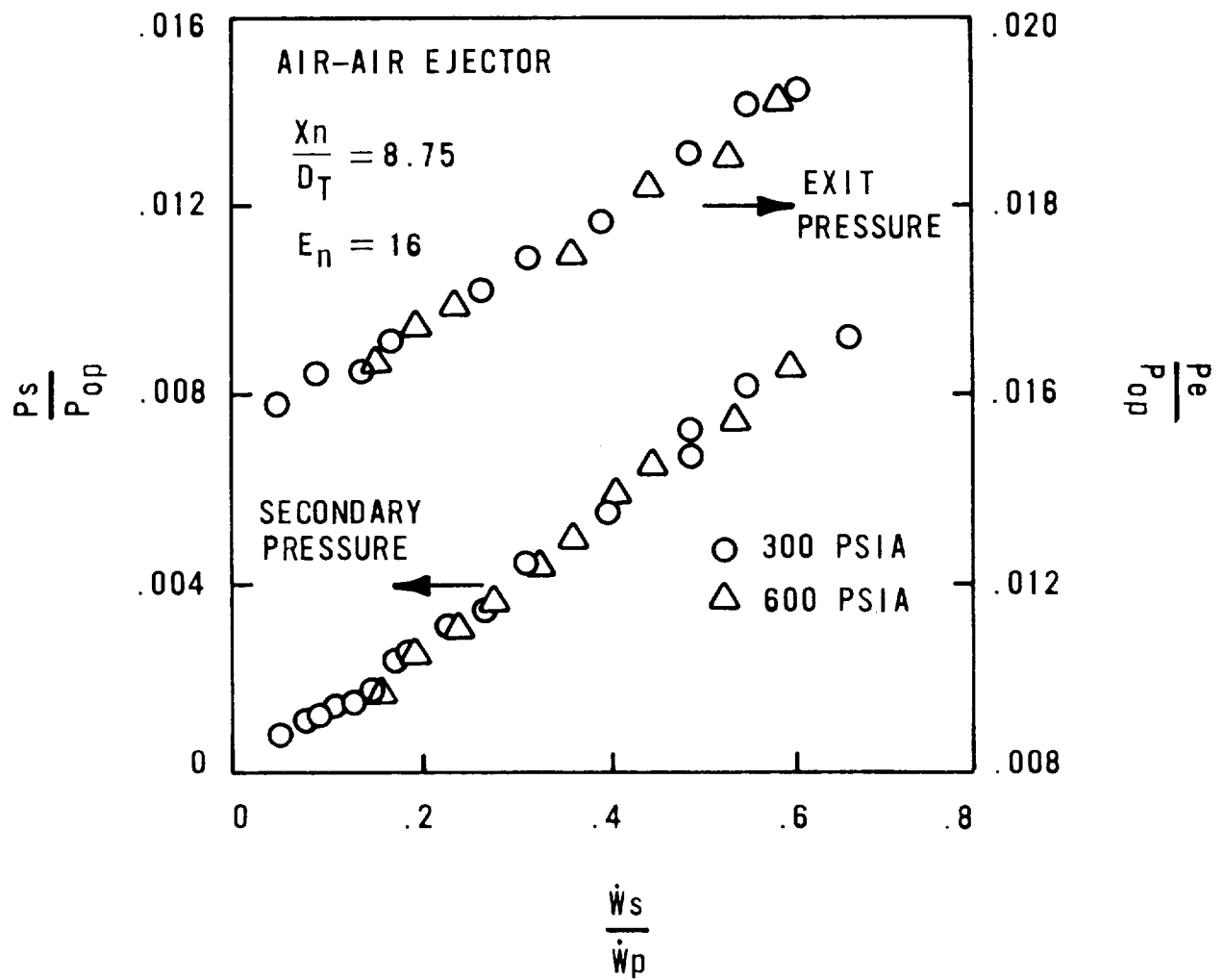


Figure 8.- Effect on secondary flow on ejector performance.

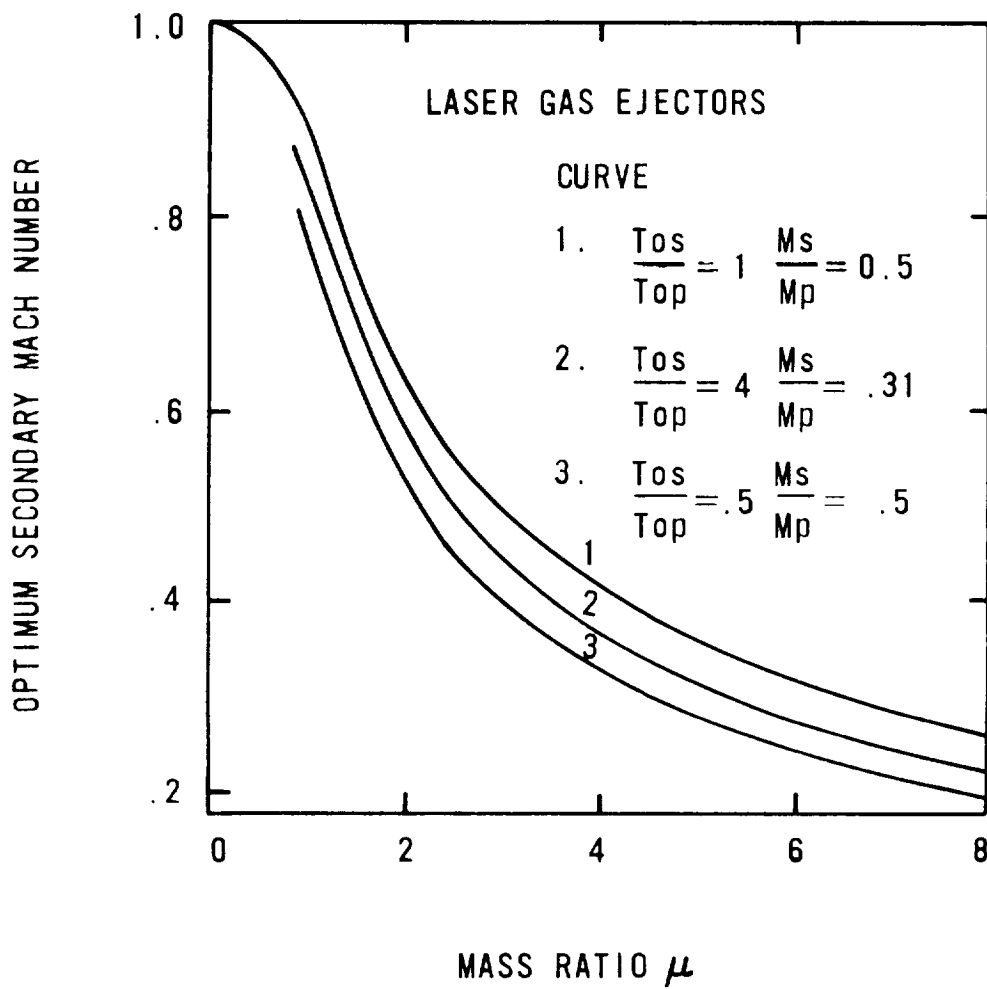


Figure 9.- Effect of mass ratio on optimum secondary Mach number.

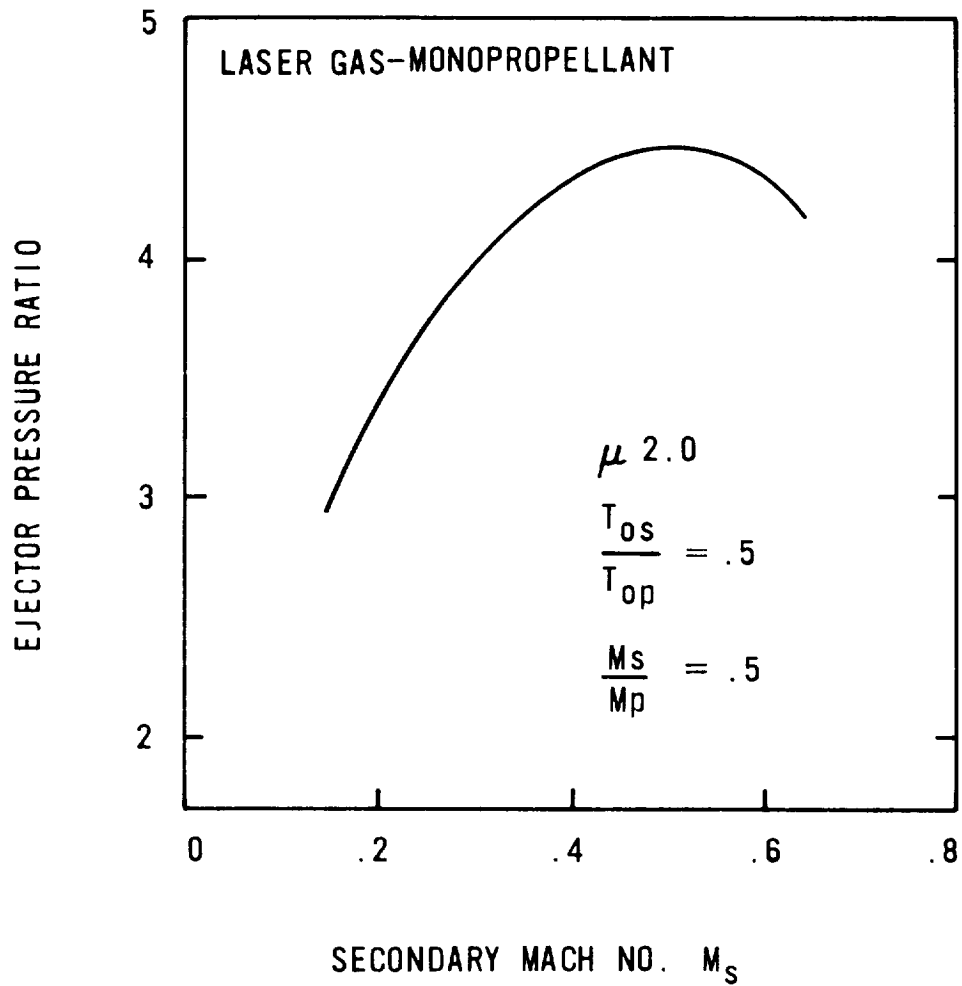


Figure 10.- Effect of optimization on ejector performance.

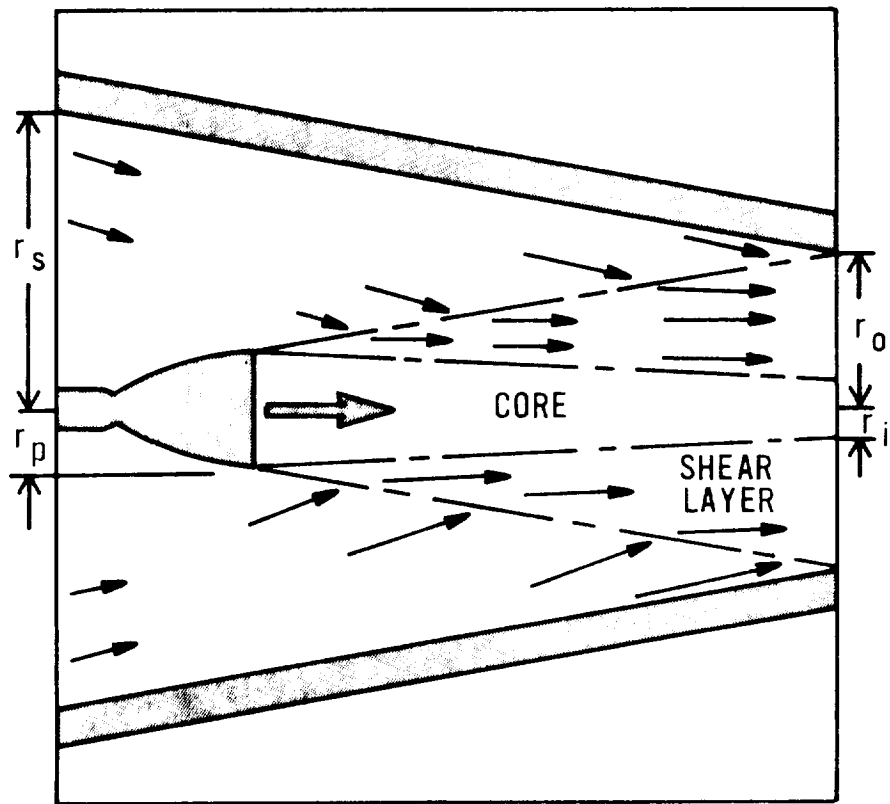


Figure 11.- Flow condition for computing throat area.

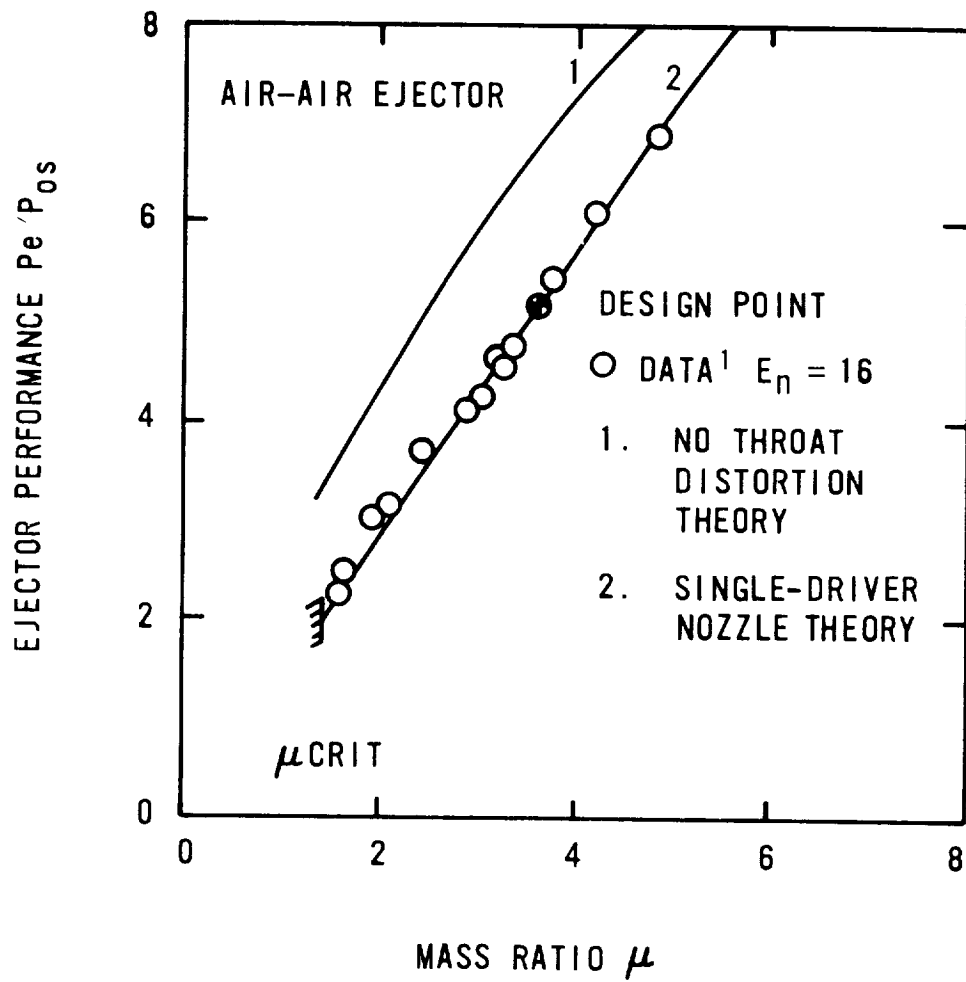


Figure 12.- Off-design ejector performance.

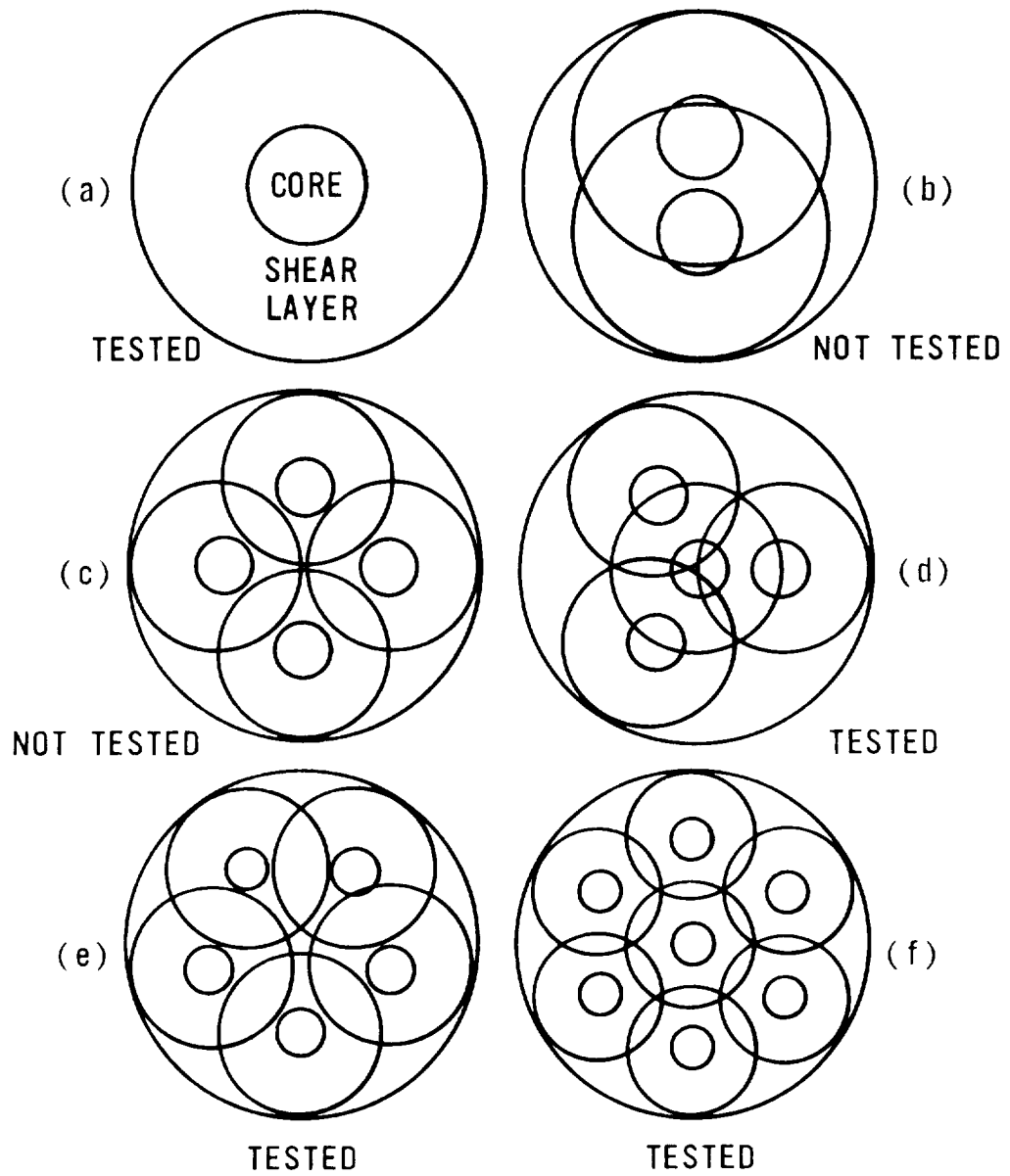


Figure 13.- Multiple-nozzle mixing zone interference.

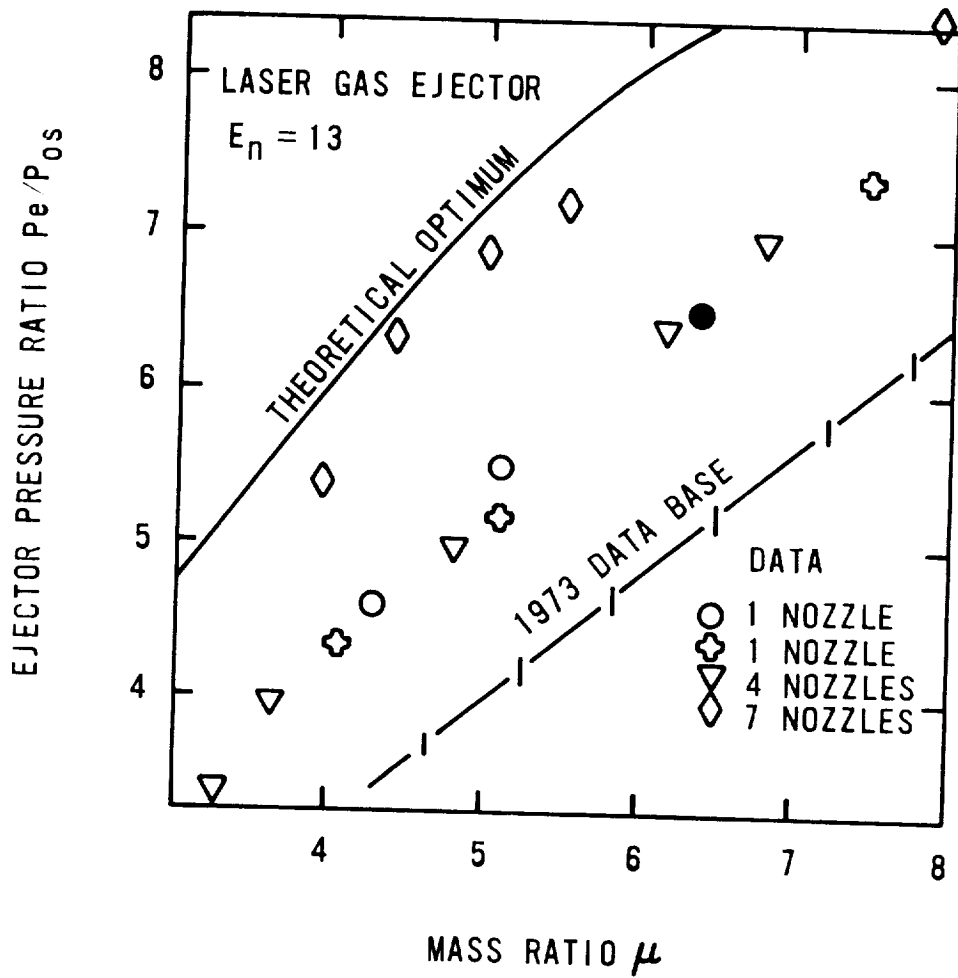


Figure 14.- Effect of number of driver nozzles on ejector performance.

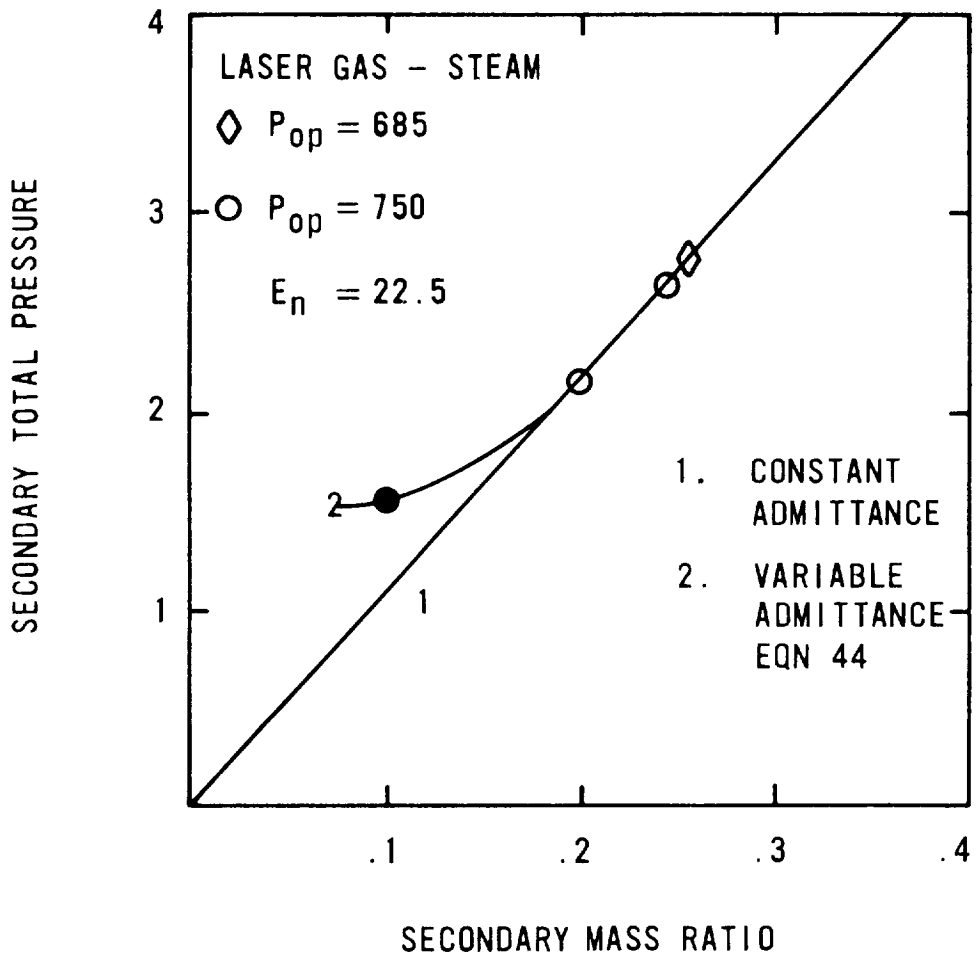


Figure 15.- Suction characteristics of multiple-driver nozzles.

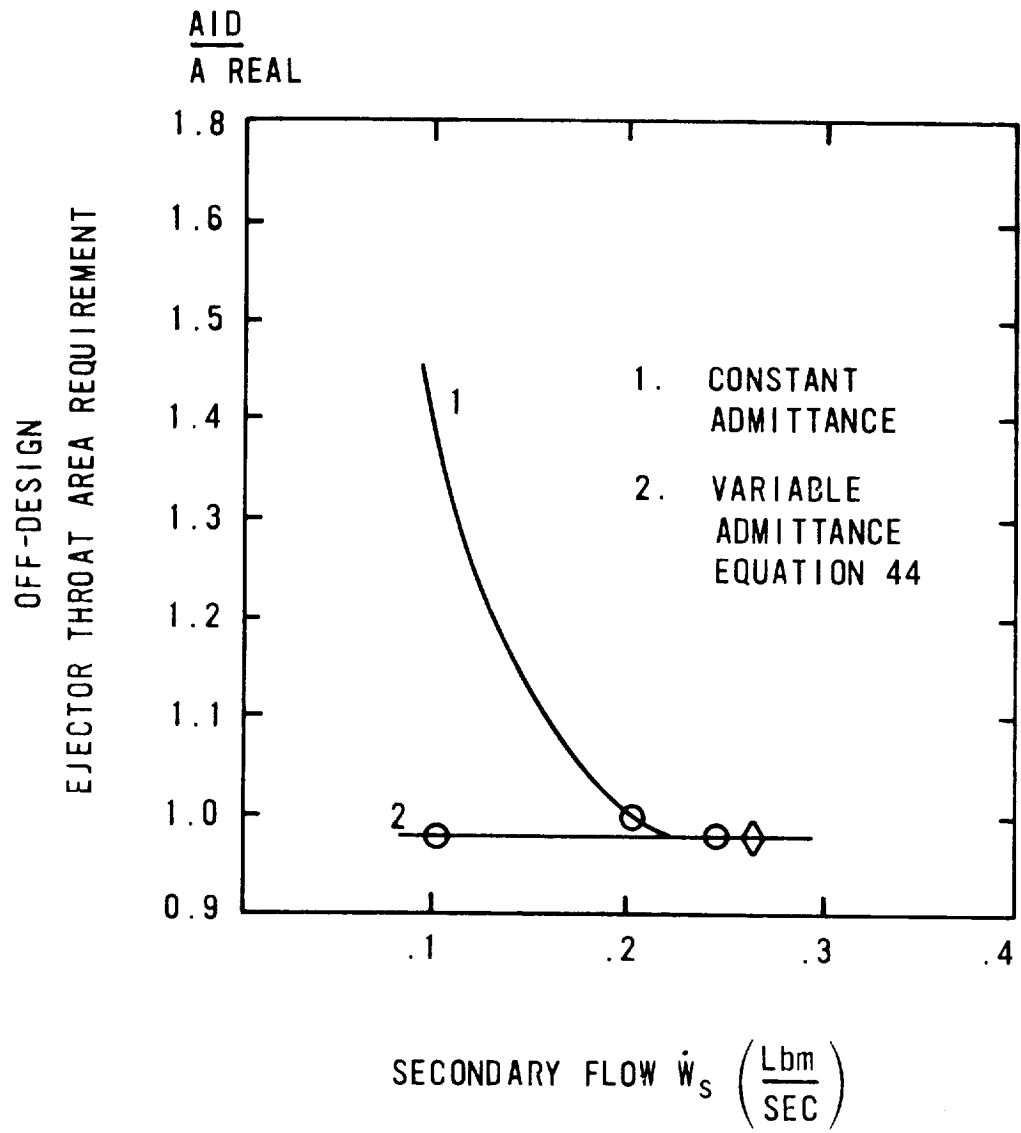


Figure 16.- Ejector area requirements.

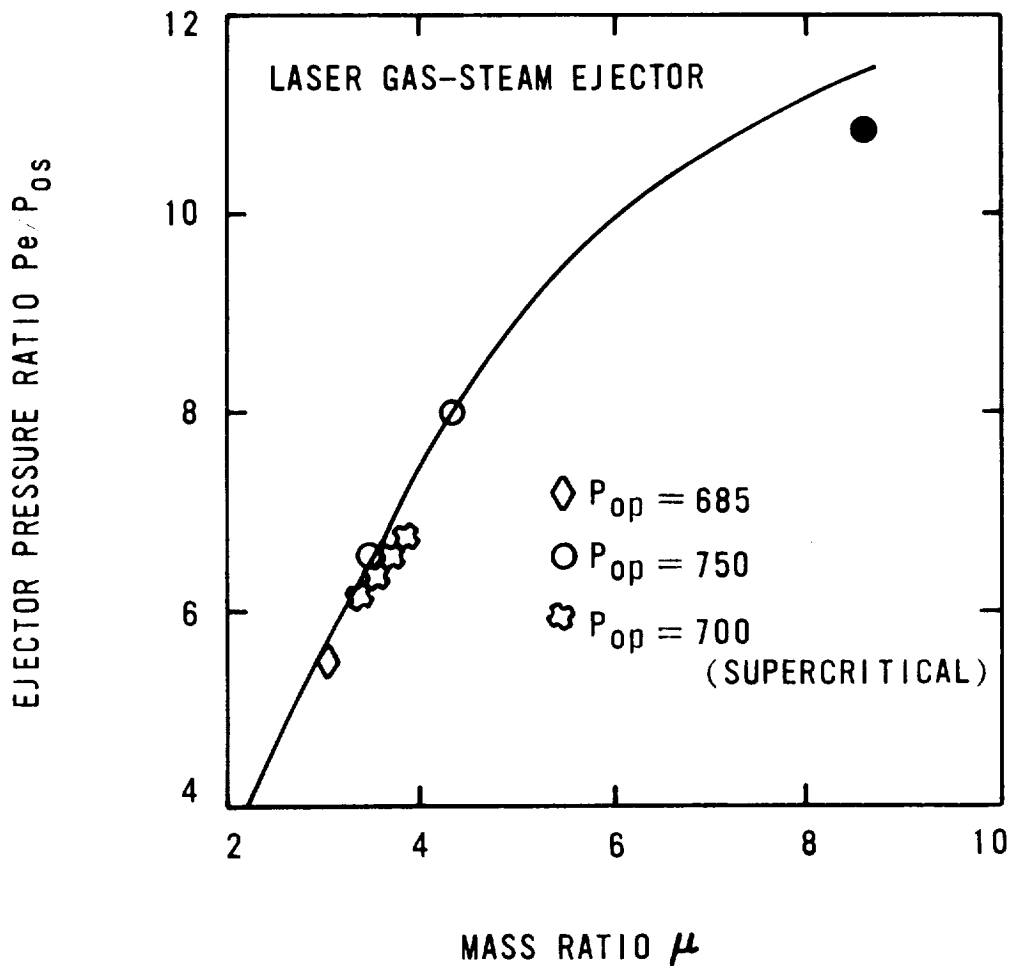


Figure 17.- Performance of multiple-driver nozzle ejector.